

Hierarchical bimetallic nitride hybrid electrode with strong electron interaction for enhanced hydrogen production in seawater

Kaihua Liu,^{†} Xinzeng Zhang,[†] Jing Li, Yuanyuan Liu, Meiri Wang, Hongtao Cui*

Shandong Engineering Research Center of Green Manufacturing for New Chemical Materials, School of Chemistry & Chemical Engineering, Yantai University, Yantai 264005, China

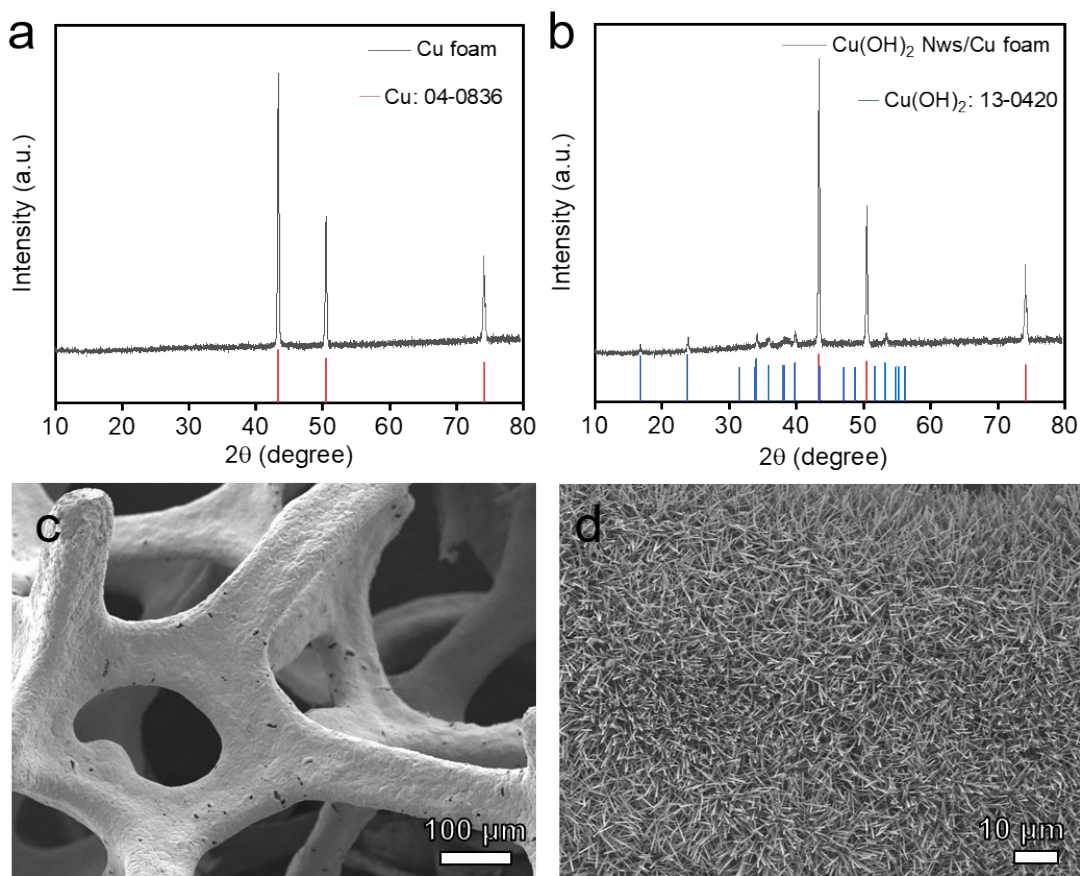


Figure S1. XRD patterns and SEM images of Cu foam (a, c) and Cu(OH)_2 nanowires integrated on Cu foam (b, d), respectively.

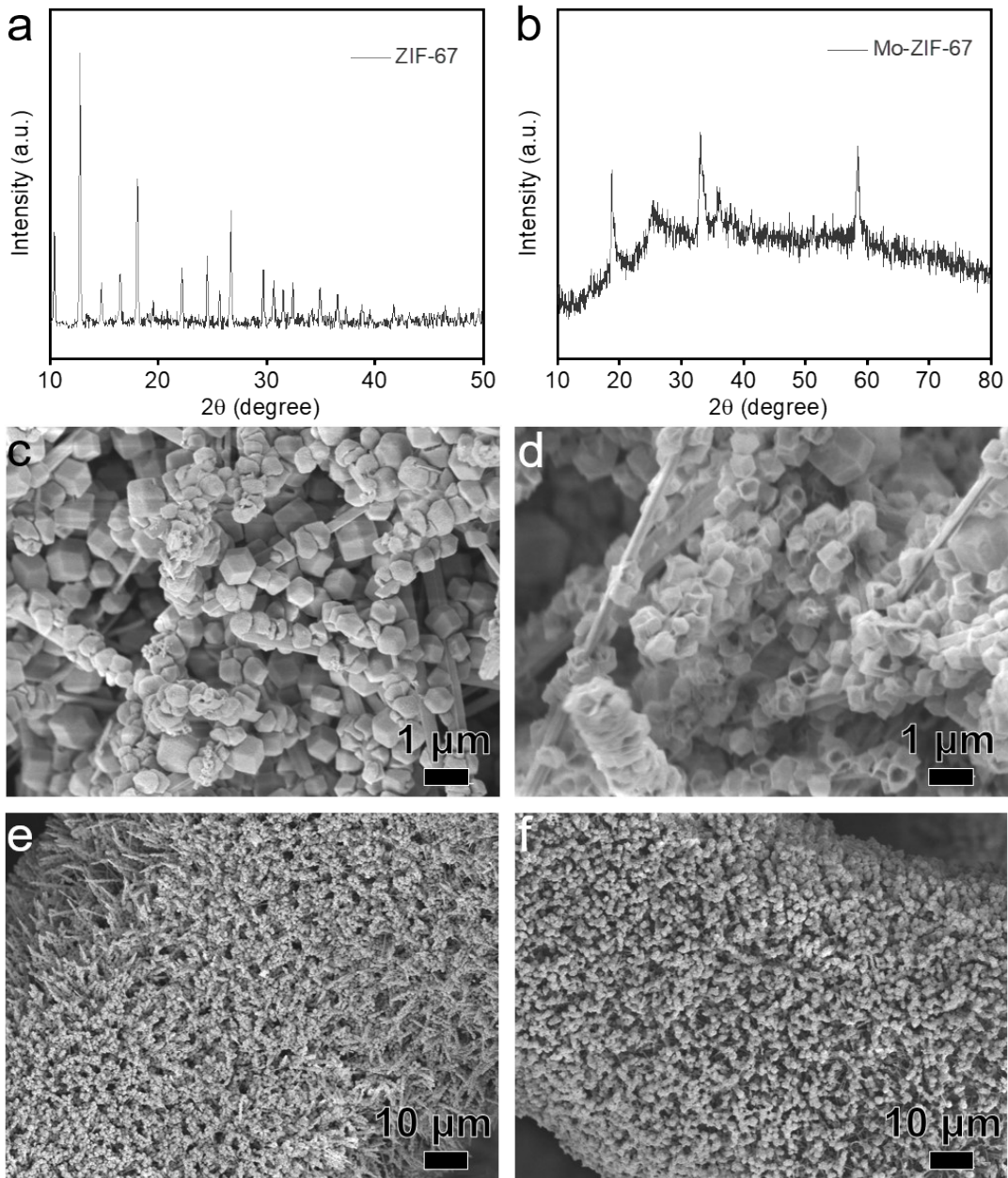


Figure S2. XRD patterns of ZIF-67 (a) and Mo-ZIF-67 (b). SEM images of ZIF-67 on $\text{Cu}(\text{OH})_2$ nanowires/Cu foam (c, e) and Mo-ZIF-67 on $\text{Cu}(\text{OH})_2$ nanowires/Cu foam (d, f), respectively.

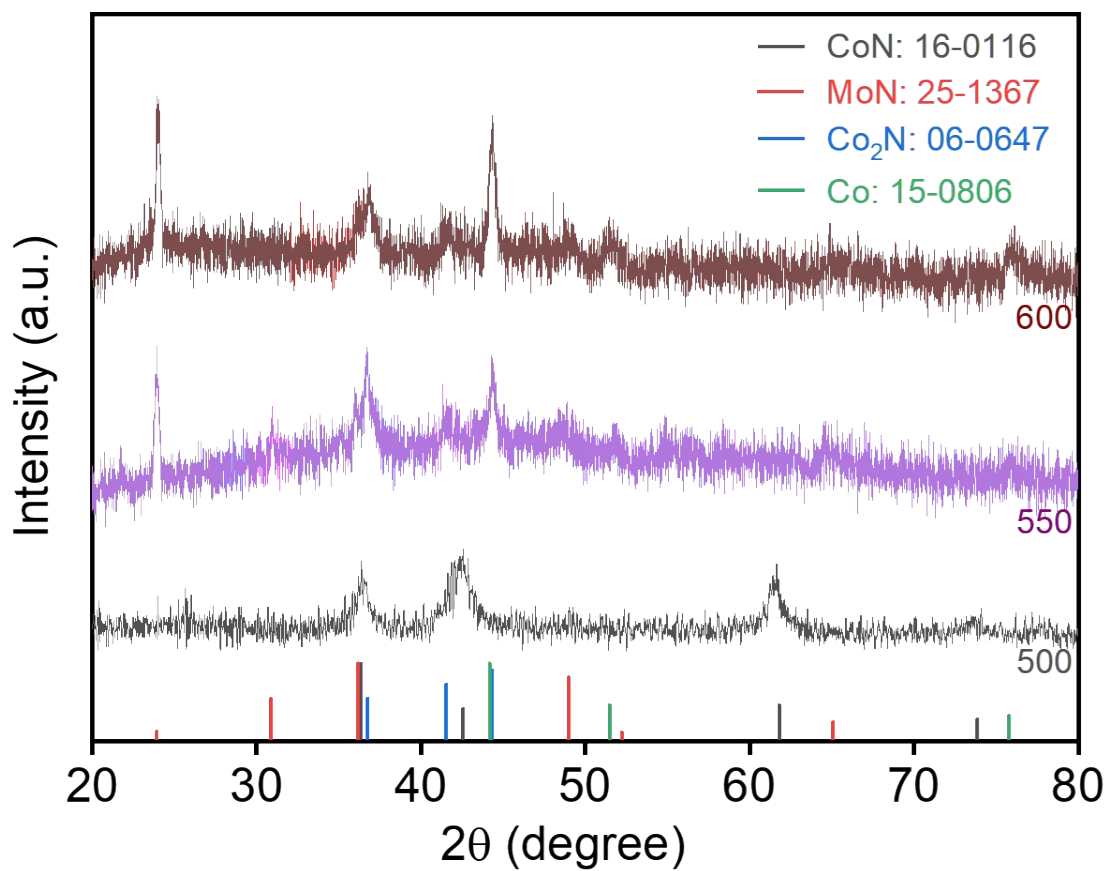


Figure S3. XRD patterns of Mo-ZIF-67 annealed at 500 °C, 550 °C, and 600 °C, respectively.

a

| | Co concentration (ppb) | Mo concentration (ppb) | Co/Mo molar ratio |
|-------------|------------------------|------------------------|-------------------|
| Co/Mo-N-C | 273291 | 564315 | 1:1 |
| Co/Mo-N-C-1 | 167119 | 462552 | 1:2 |
| Co/Mo-N-C-2 | 288392 | 305485 | 2:1 |

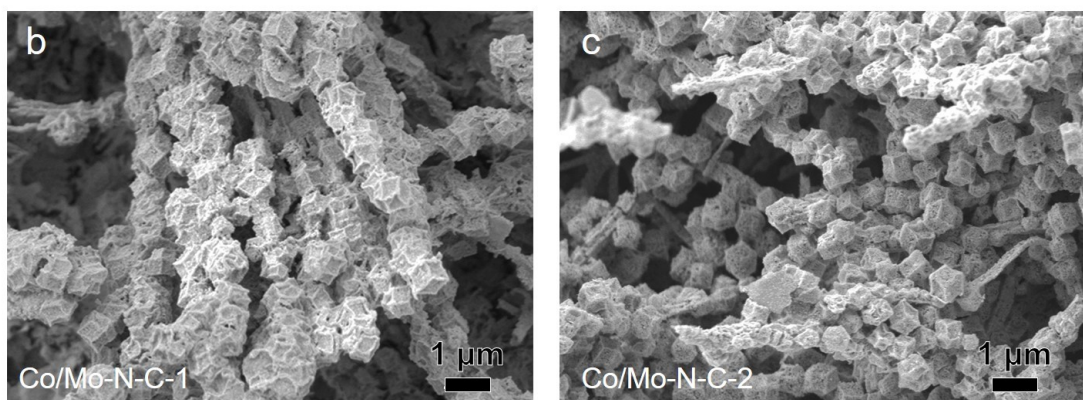


Figure S4. ICP-OES results of the prepared Co/Mo-N-C electrodes (a). SEM images of Co/Mo-N-C electrodes with different Co/Mo molar ratio (b, c).

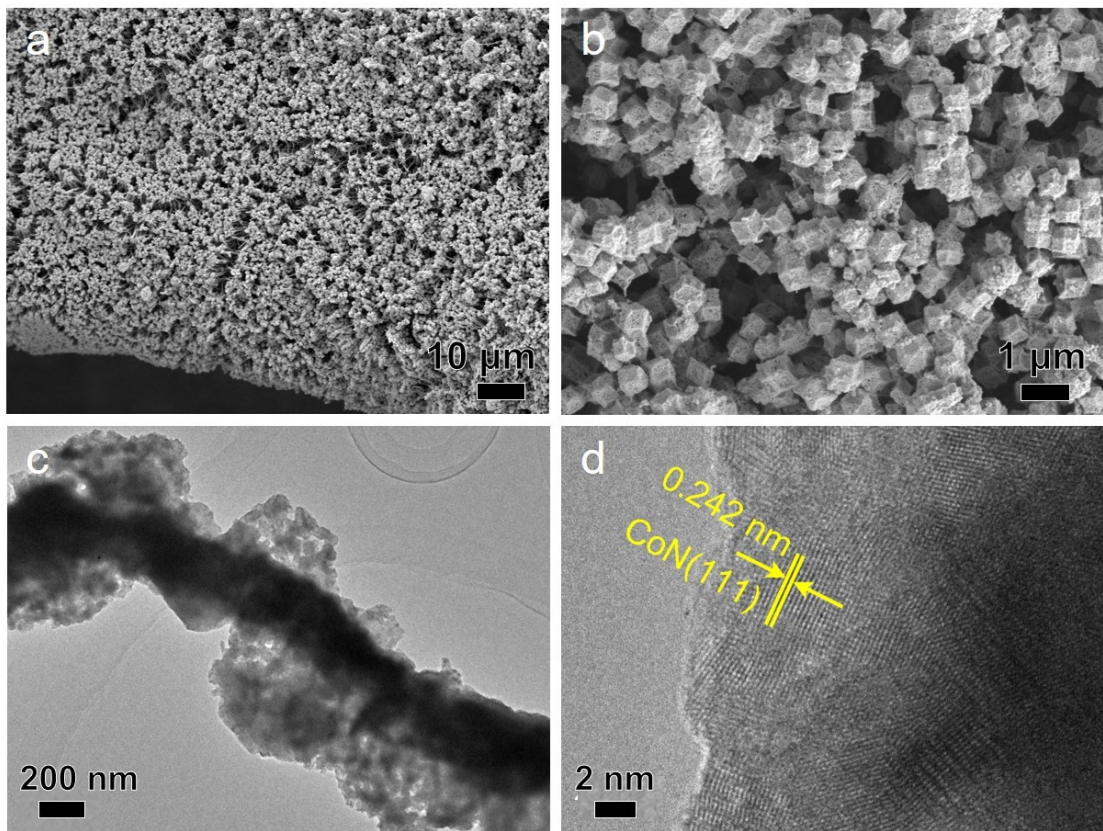


Figure S5. SEM images (a, b), TEM image (c) and HRTEM image (d) of Co/Mo-N-C/Cu electrode annealed at 500 °C.

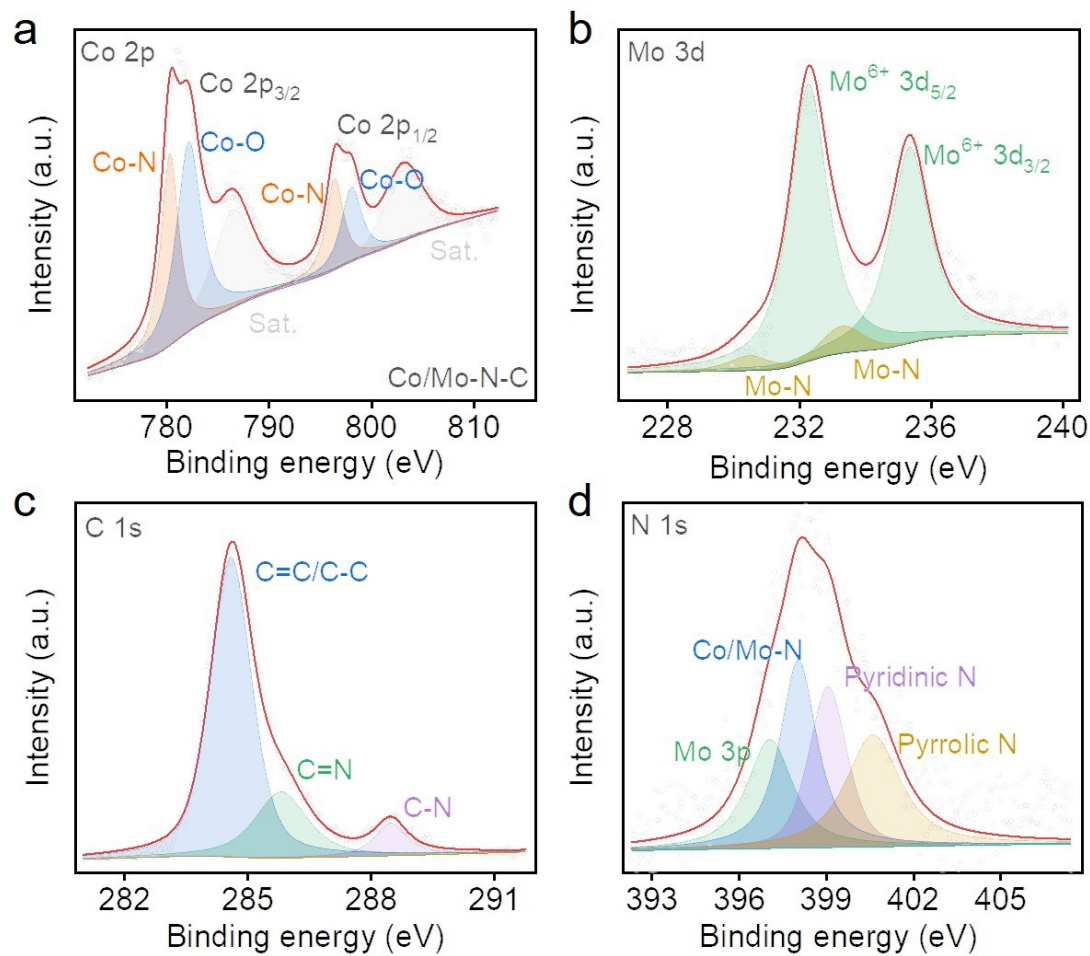


Figure S6. High-resolution Co 2p (a), Mo 3d (b), C 1s (c), and N 1s (d) XPS spectra of Co/Mo-N-C/Cu electrode annealed at 500 °C.

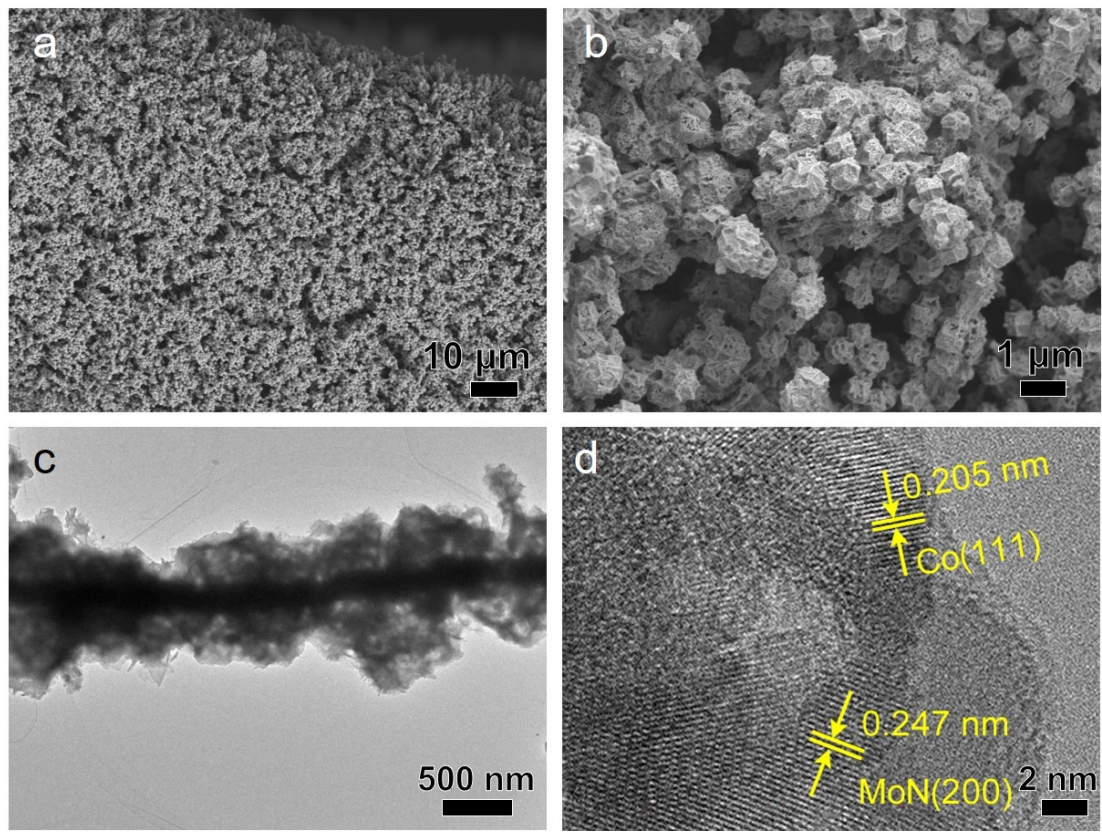


Figure S7. SEM images (a, b), TEM image (c) and HRTEM image (d) of Co/Mo-N-C/Cu electrode annealed at 600 °C.

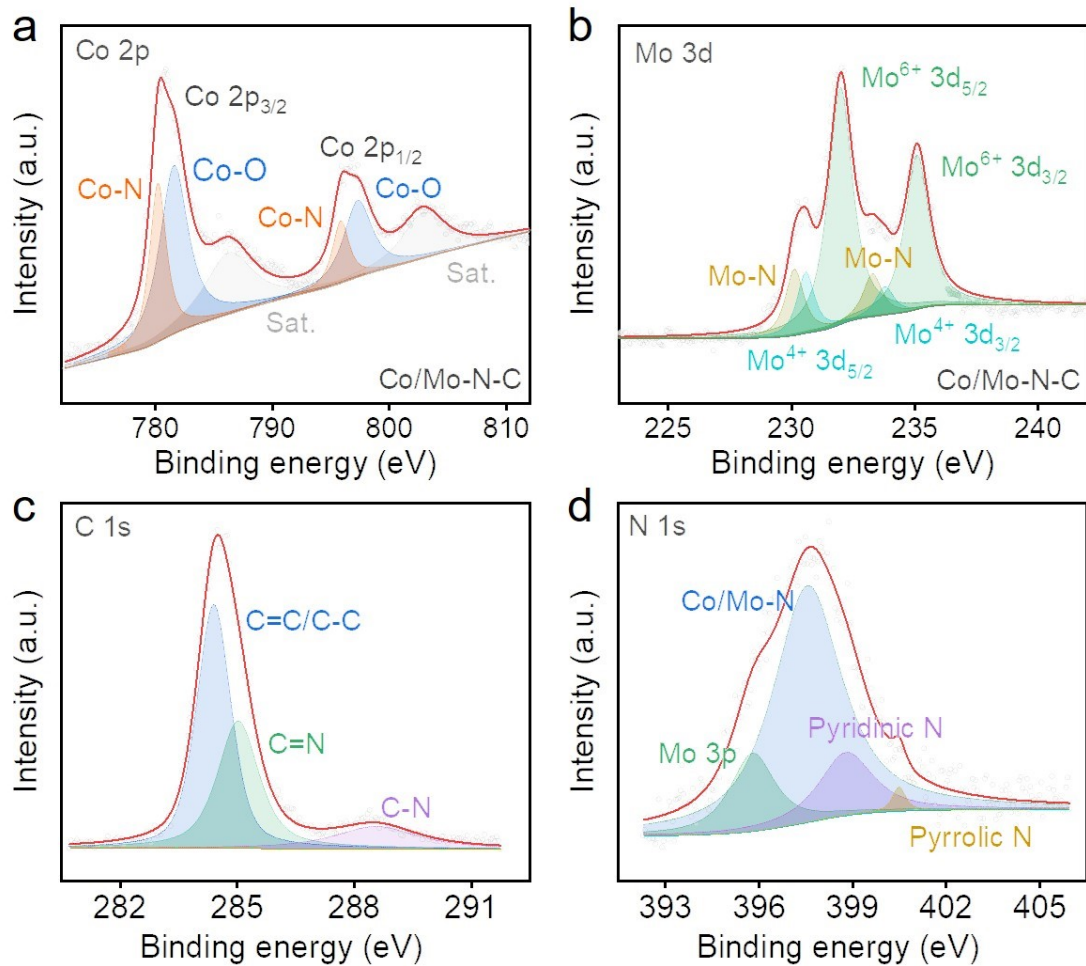


Figure S8. High-resolution Co 2p (a), Mo 3d (b), C 1s (c), and N 1s (d) XPS spectra of Co/Mo-N-C/Cu electrode annealed at 600 °C.

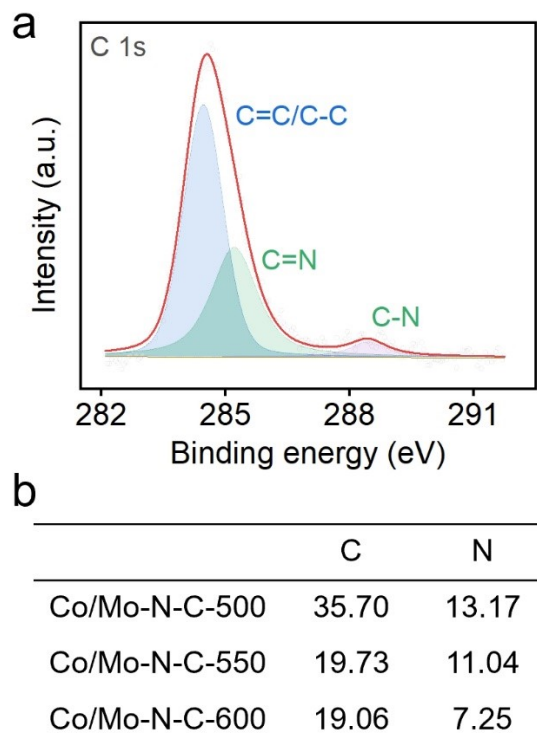


Figure S9. High-resolution XPS spectrum of C 1s (a) in the Co/Mo-N-C electrode, and N and C content (Atomic%) in the samples based on XPS (b).

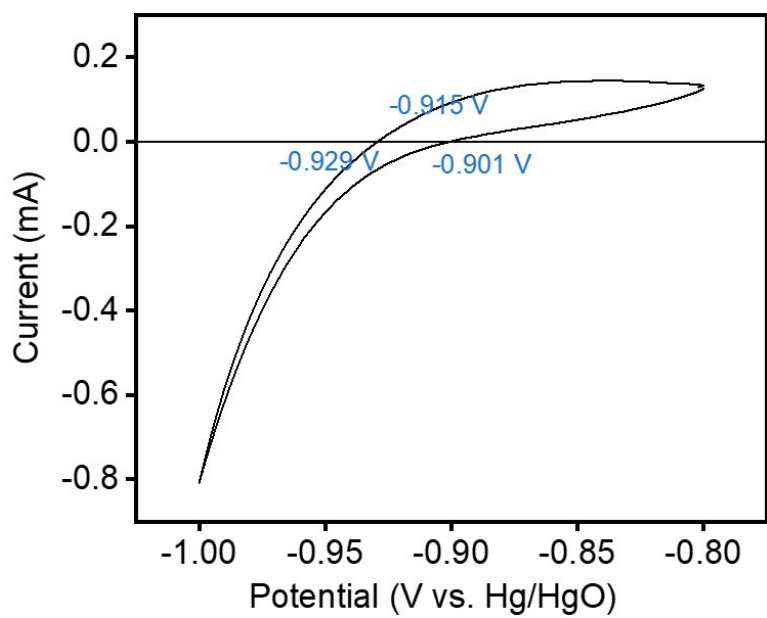


Figure S10. Current-potential curve of Pt plate as the working electrode in H_2 -saturated seawater with 1 M KOH solution to calibrate the Hg/HgO electrode with respect to RHE, $E_{\text{RHE}} = E_{\text{Hg/HgO}} + 0.915 \text{ V}$.

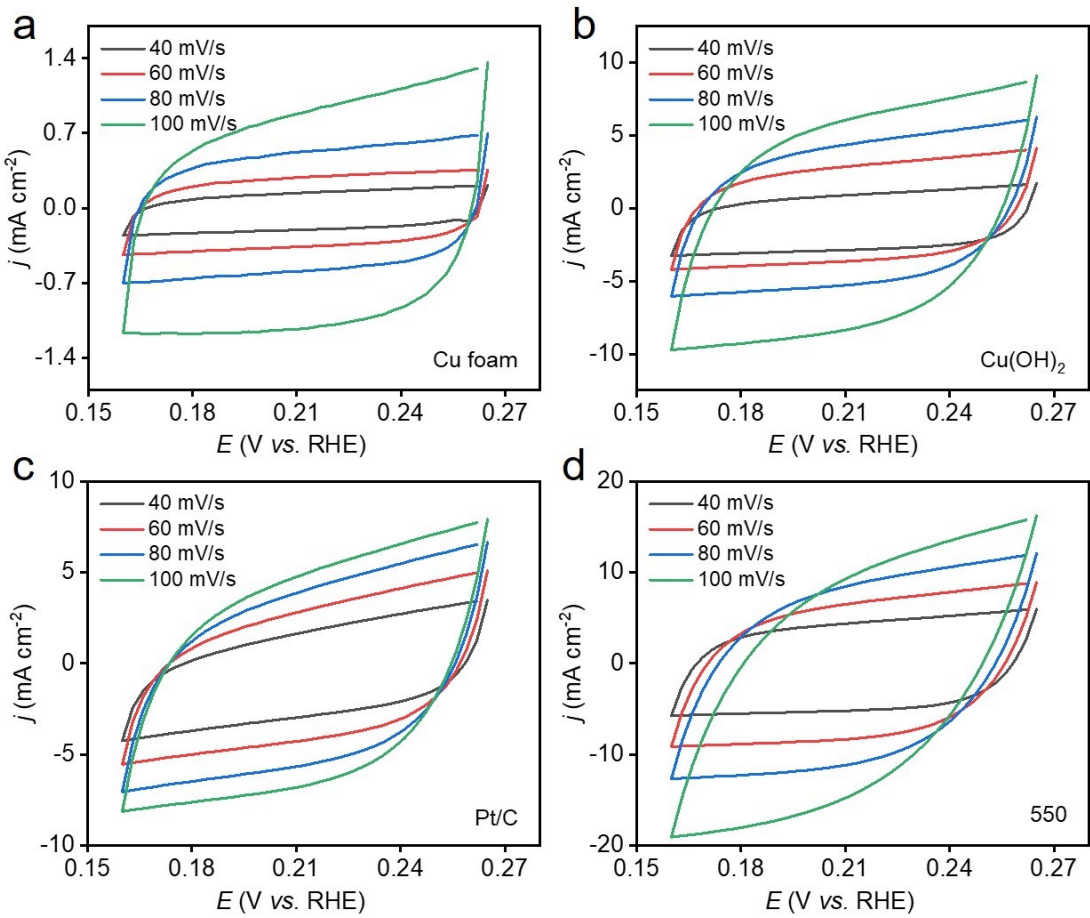


Figure 11. Cyclic voltammograms in the potential windows ranging from 0.16 V to 0.26 V for Cu foam (a), Cu(OH)₂ nanowires/Cu foam (b), Pt/C/Cu foam (c) and Co/Mo-N-C/Cu annealed at 550 °C (d) at various scan rates.

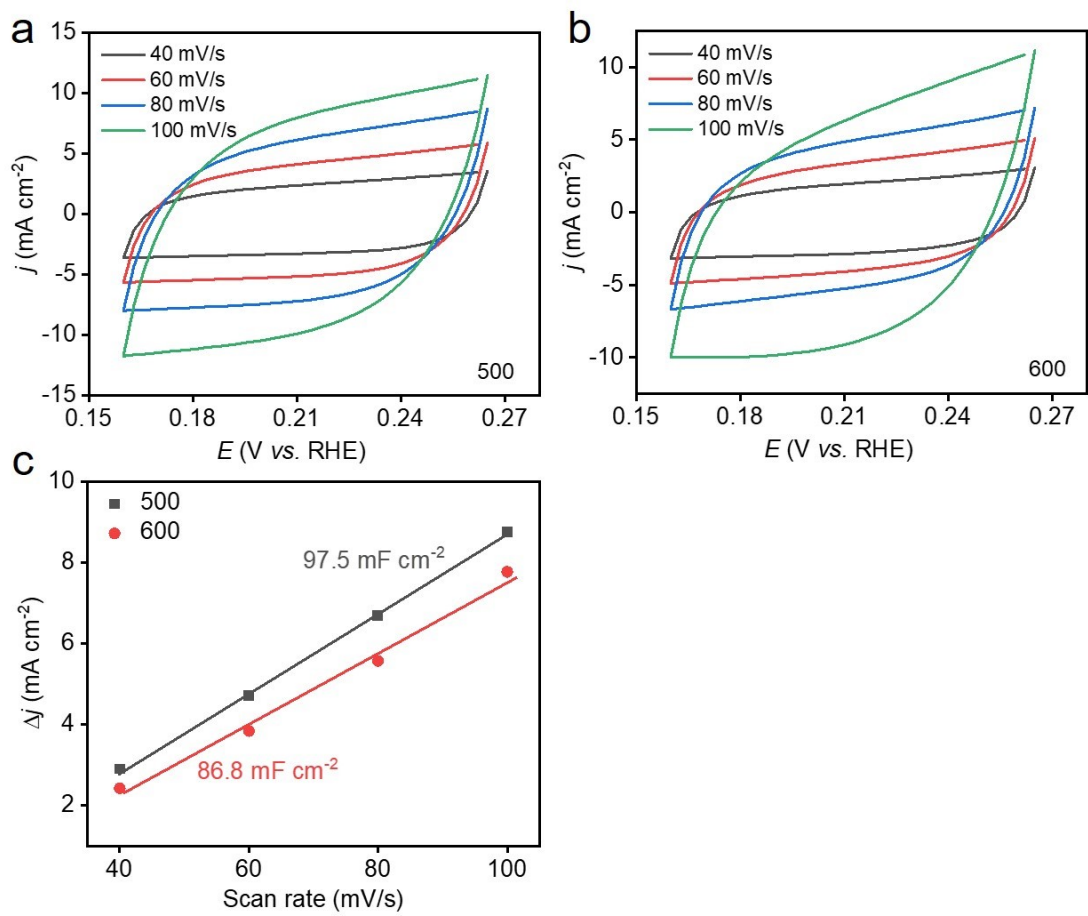


Figure 12. Cyclic voltammograms in the potential windows ranging from 0.16 V to 0.26 V for Co/Mo-N-C/Cu annealed at 500 °C (a) and 600 °C (b) at various scan rates. The calculated double-layer capacitances (c).

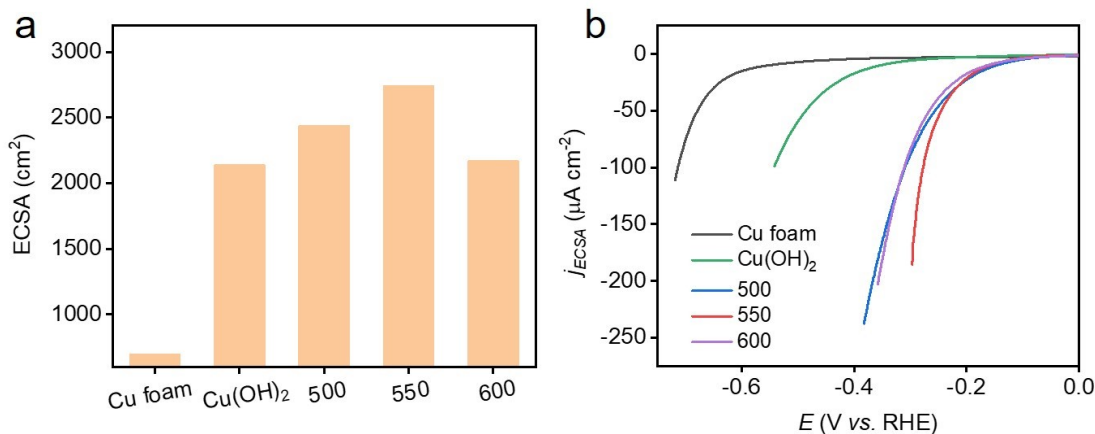


Figure 13. Electrochemical surface areas (a) and specific activities (b) of Cu foam, Cu(OH)₂ nanowires/Cu, and Co/Mo-N-C/Cu electrodes annealed at 500 °C, 550 °C and 600 °C, respectively.

The electrochemical active surface area (ECSA) was estimated by electrochemical double layer capacitance (C_{dl}). In detail, by plotting the Δj ($j_a - j_c$) at 0.226 V against the scan rates, the slope of the straight line obtained by fitting Δj at different scan rates was used to evaluate the magnitude of the capacitance, which was positively correlated with ECSA. This can be expressed by the following equation:

$$ECSA = \frac{C_{dl}}{40 \mu F cm^{-2}} * S$$

The specific capacitance for a flat surface we used is an average of 40 μF cm⁻².

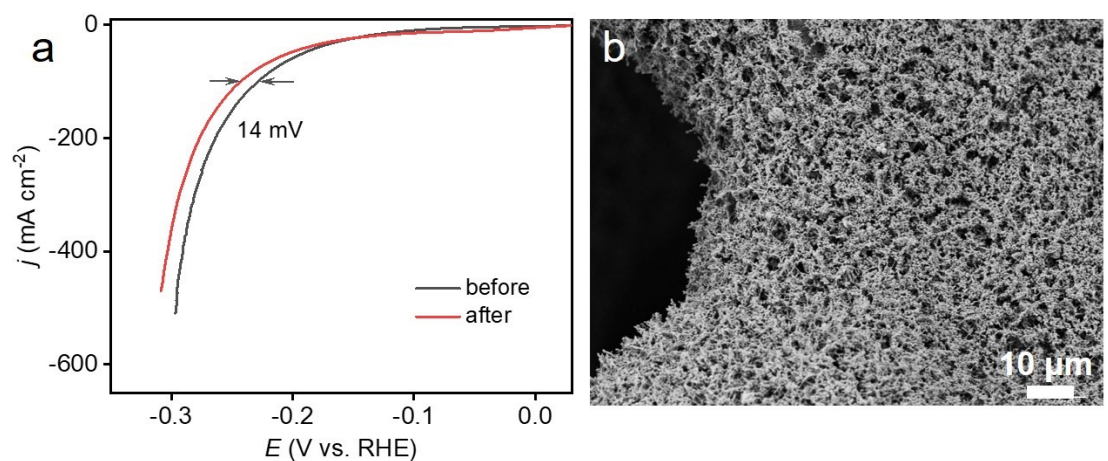


Figure 14. Polarization curves before and after HER stability test (a) and SEM image of Co/Mo-N-C/Cu electrode after the HER stability test (b).

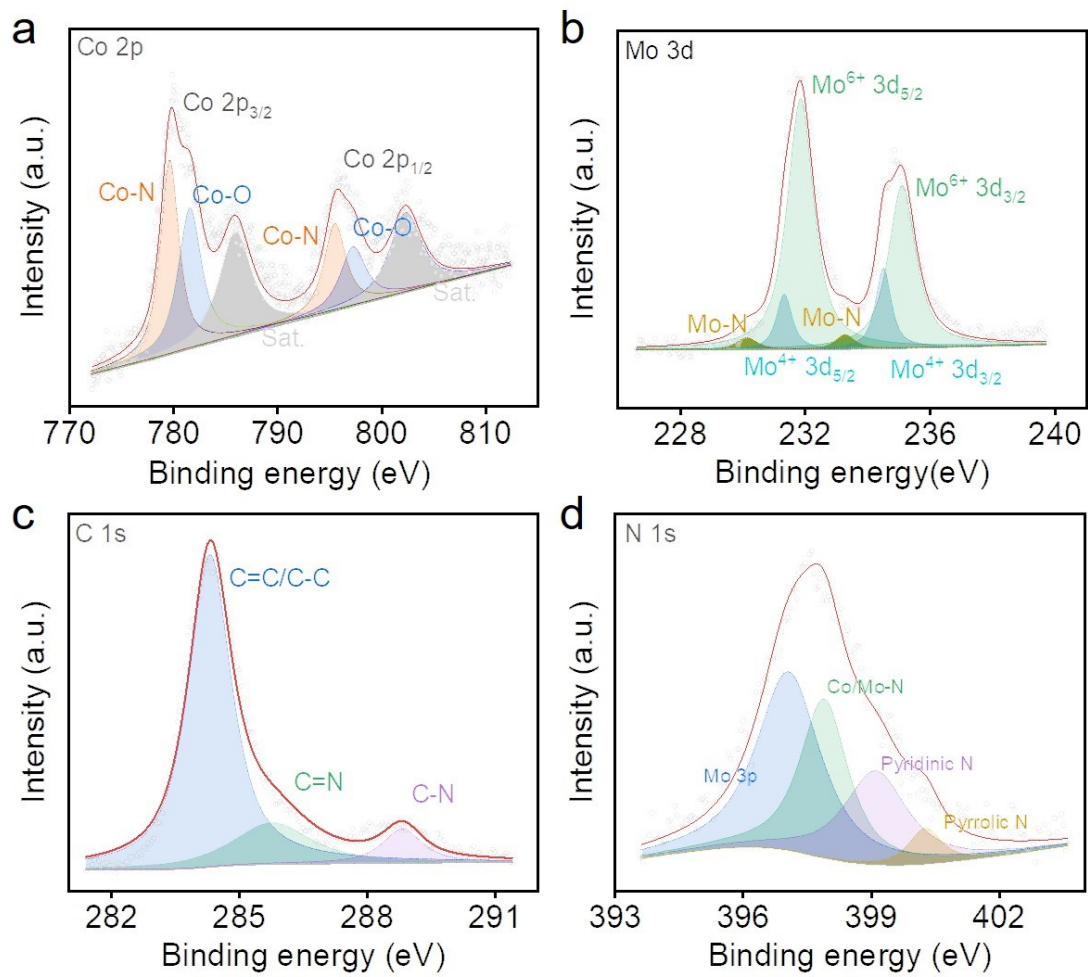


Figure 15. High-resolution Co 2p (a), Mo 3d (b), C 1s (c) and N 1s (d) XPS spectra of Co/Mo-N-C/Cu electrode after the HER stability test.

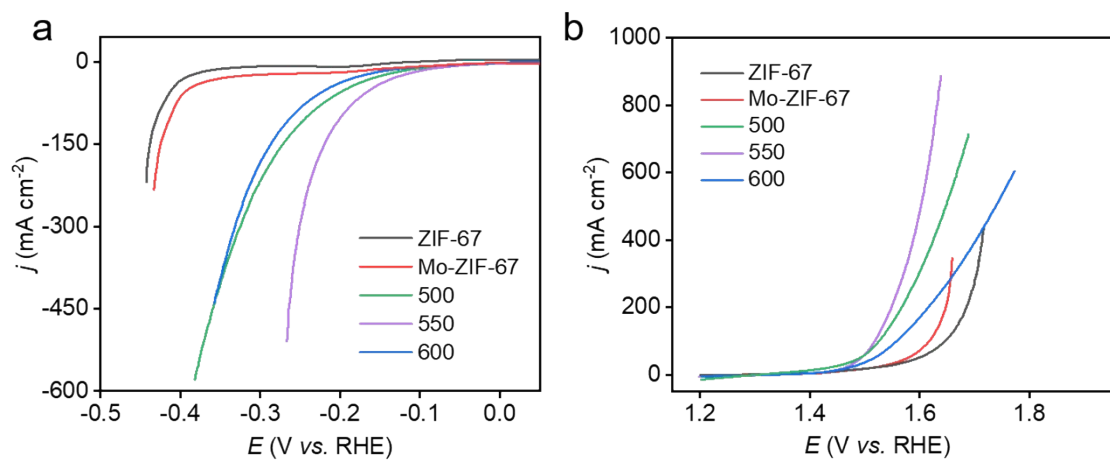


Figure 16. Typical HER (a) and OER (b) polarization curves of ZIF-67/Cu, Mo-ZIF-67/Cu and Co/Mo-N-C/Cu electrode annealed at 500 °C, 550 °C, and 600 °C, respectively.

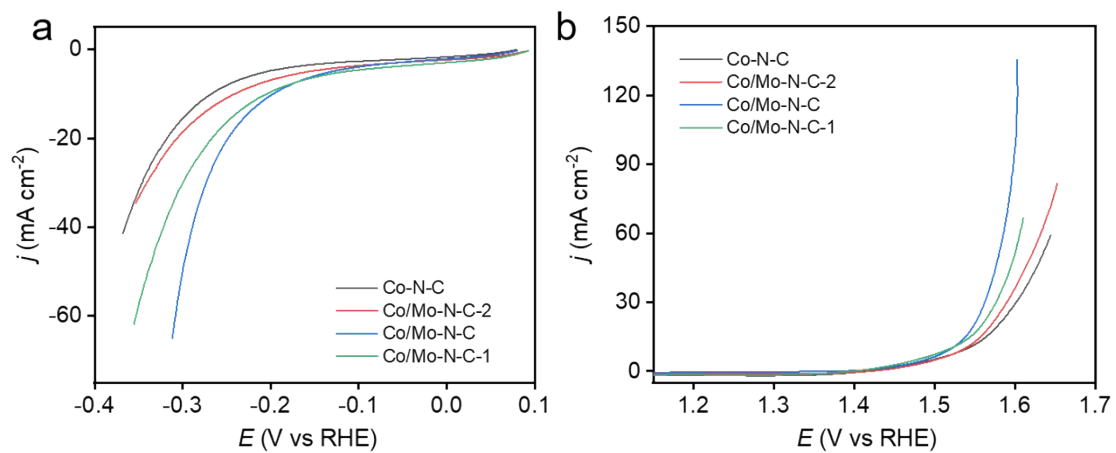


Figure 17. Typical HER (a) and OER (b) polarization curves of Co/Mo-N-C/Cu electrode with different Co/Mo atom ratio.

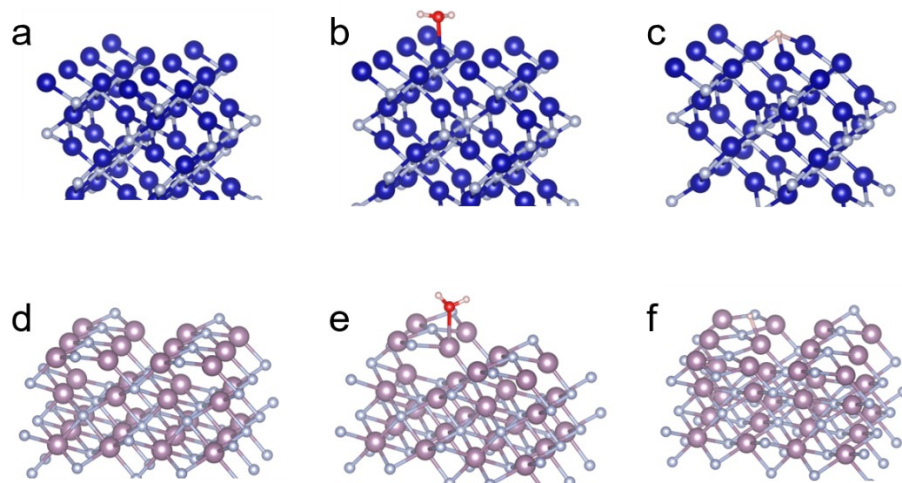


Figure 18. Atomic structure (a) and surface configurations of H₂O (b) and H (c) adsorption on Co₂N (002). Atomic structure (d) and surface configurations of H₂O (e) and H (f) adsorption on MoN (200).

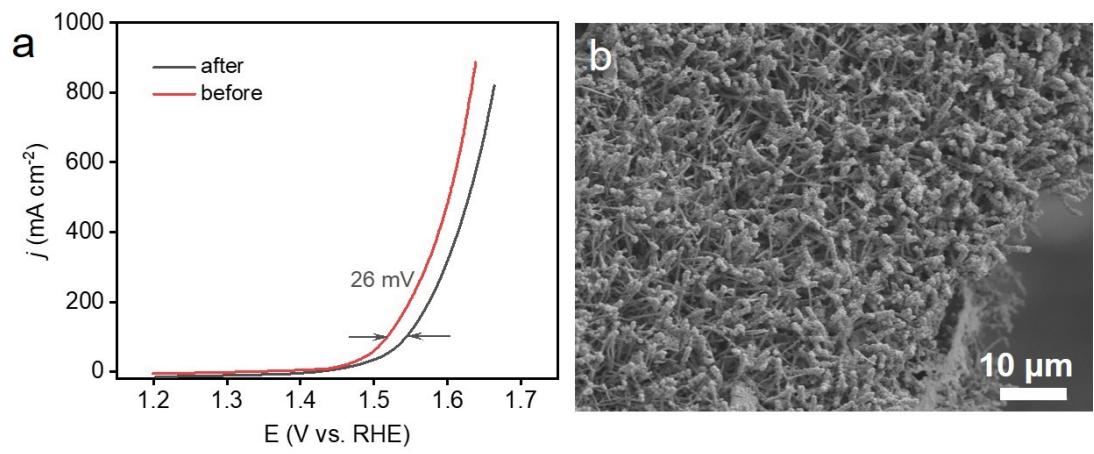


Figure 19. Polarization curves before and after OER stability test (a) and SEM image of Co/Mo-N-C/Cu electrode after the OER stability test (b).

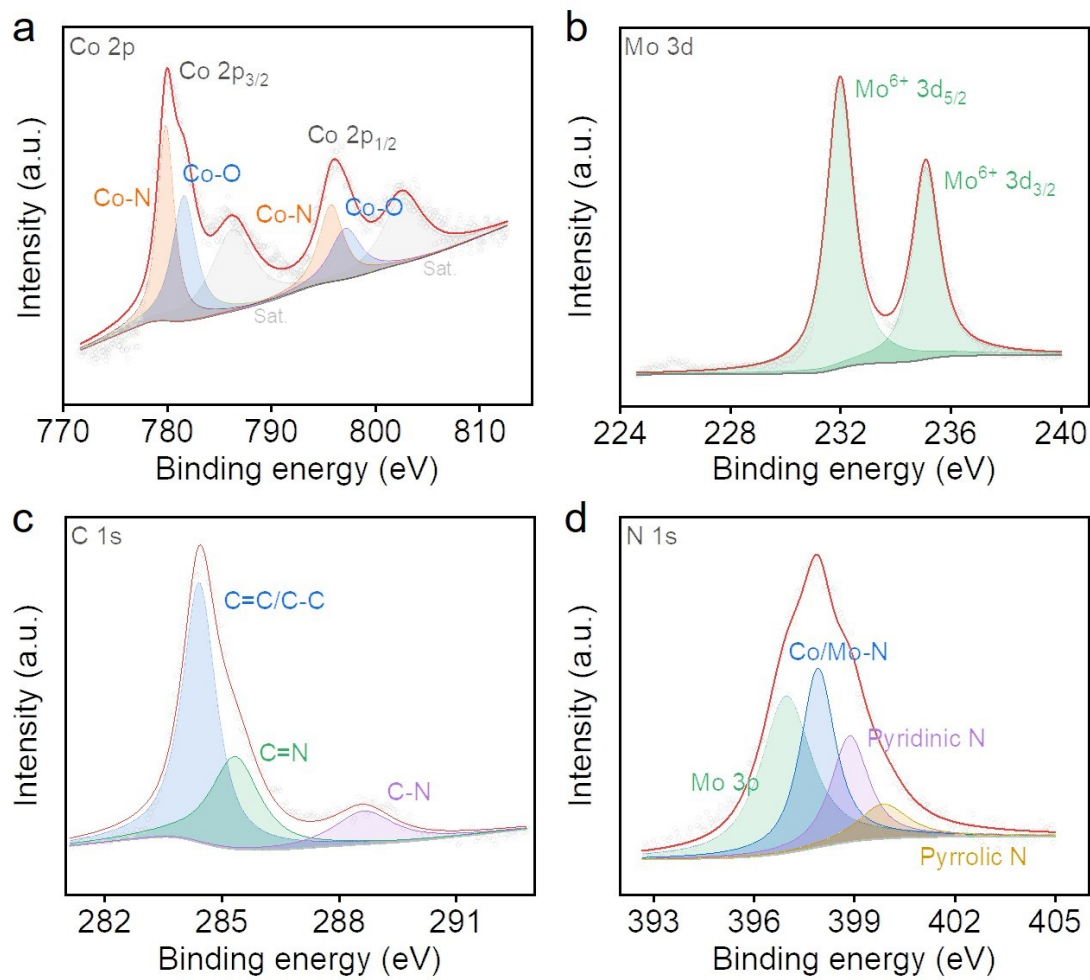


Figure 20. High-resolution Co 2p (a), Mo 3d (b), C 1s (c) and N 1s (d) XPS spectra of Co/Mo-N-C/Cu electrode after the OER stability test.

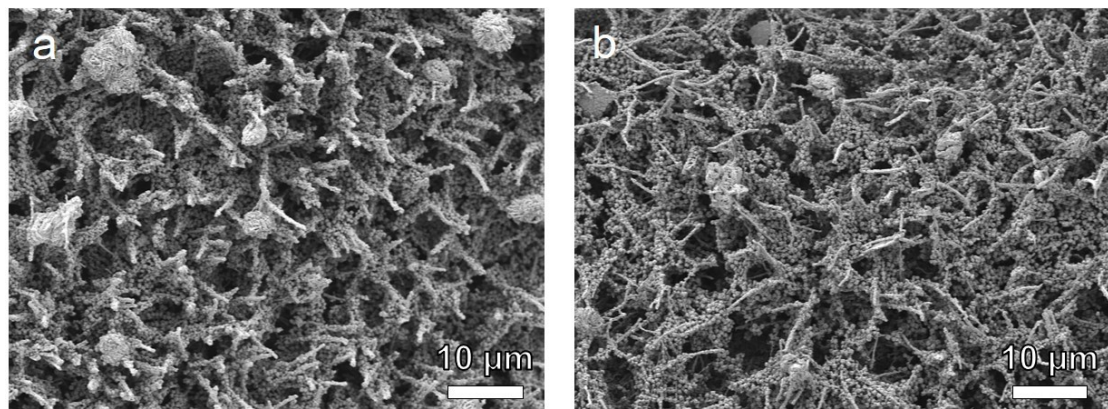


Figure 21. SEM images of Co/Mo-N-C/Cu cathode (a) and Co/Mo-N-C/Cu anode (b) after the stability measurement of overall water splitting.

Table S1. Comparisons of the overall seawater splitting performance of Co/Mo-N-C/Cu||Co/Mo-N-C/Cu with representative electrocatalysts reported previously.

| Electrocatalysts | Electrolyte | η (V) at 100 mA cm ⁻² | Reference |
|---|---------------------------|---------------------------------------|------------------|
| Co/Mo-N-C/Cu Co/Mo-N-C/Cu | Seawater + 1 M KOH | 1.70 | This work |
| Cr-Co _x P Cr-Co _x P | Seawater + 1 M KOH | 1.85 | [1] |
| Ni ₂ P-Fe ₂ P/NF Ni ₂ P-Fe ₂ P/NF | Seawater + 1 M KOH | 1.81 | [2] |
| B-MnFe ₂ O ₄ B-MnFe ₂ O ₄ | Seawater + 1 M KOH | 1.8 | [3] |
| FCNP@CQDs/CP FCNP@CQDs/CP | Seawater + 1 M KOH | 1.78 | [4] |
| Pt ₂ /Ni(OH) ₂ /NF Pt ₂ /Ni(OH) ₂ /NF | Seawater + 1 M KOH | 1.9 | [5] |
| Co ₃ Mo/Cu Co ₃ Mo/Cu | 1 M KOH + 0.5 M NaCl | 1.62 | [6] |
| Ni/ γ -Fe ₂ O ₃ Ni/ γ -Fe ₂ O ₃ | 1 M KOH | 1.77 | [7] |
| CoP-InNC CoP-InNC | 1 M KOH | 1.86 | [8] |
| FeNiS/Ni FeNiS/Ni | 1 M KOH | 1.82 | [9] |
| FeCoNi/CC FeCoNi/CC | 1 M KOH | 2.0 | [10] |
| Cu ₃ N Cu ₃ N | 1 M KOH | 1.80 | [11] |
| NiFe-LDH@NiCu NiFe-LDH@NiCu | 1 M KOH | 1.84 | [12] |
| CO ₃ S ₄ /MOF CO ₃ S ₄ /MOF | 1 M KOH | 1.9 | [13] |
| NiFeSe NiFeSe | 1 M KOH | 1.86 | [14] |
| CoMoNiS CoMoNiS | 1 M KOH | 2.09 | [15] |
| Ir/MoS ₂ Ir/MoS ₂ | 1 M KOH | 1.78 | [16] |
| PSCoO/Cu@CuS PSCoO/Cu@CuS | 1 M KOH | 2.0 | [17] |
| O-CoP O-CoP | 1 M KOH | 1.79 | [18] |
| NiCo ₂ S ₄ NiCo ₂ S ₄ | 1 M KOH | 1.95 | [19] |
| CoNC CoNC | 1 M KOH | 1.86 | [20] |
| NiFe@Ni NiFe@Ni | 1 M KOH | 1.83 | [21] |
| FeCo/Co ₂ P@C FeCo/Co ₂ P@C | 1 M KOH | 1.98 | [22] |
| CoFeZr oxides CoFeZr oxides | 1 M KOH | 1.78 | [23] |
| Ni-ZIF/NiB Ni-ZIF/NiB | 1 M KOH | 1.77 | [24] |
| CoNSC CoNSC | 1 M KOH | 1.75 | [25] |
| CoP/NC CoP/NC | 1 M KOH | 1.9 | [26] |

References

- [1] Y. Song, M. Sun, S. Zhang, X. Zhang, P. Yi, J. Liu, B. Huang, M. Huang, L. Zhang, *Adv. Funct. Mater.* **2023**, 33, 2214081.
- [2] L. Wu, L. Yu, F. Zhang, B. McElhenny, D. Luo, A. Karim, S. Chen, Z. Ren, *Adv. Funct. Mater.* **2020**, 31, 2006484.
- [3] M. Chen, N. Kitiphatpiboon, C. Feng, Q. Zhao, A. Abudula, Y. Ma, K. Yan, G. Guan, *Appl. Catal. B: Environ.* **2023**, 330, 122577.
- [4] S. Lv, Y. Deng, Q. Liu, Z. Fu, X. Liu, M. Wang, Z. Xiao, B. Li, L. Wang, *Appl. Catal. B: Environ.* **2023**, 326, 122403.
- [5] J. Sun, Z. Zhang, X. Meng, *Appl. Catal. B: Environ.* **2023**, 331, 122703.
- [6] H. Shi, Y. T. Zhou, R. Q. Yao, W. B. Wan, X. Ge, W. Zhang, Z. Wen, X. Y. Lang, W. T. Zheng, Q. Jiang, *Nat. Commun.* **2020**, 11, 2940.
- [7] B. H. R. Suryanto, Y. Wang, R. K. Hocking, W. Adamson, C. Zhao, *Nat. Commun.* **2019**, 10, 5599.
- [8] L. Chai, Z. Hu, X. Wang, Y. Xu, L. Zhang, T. T. Li, Y. Hu, J. Qian, S. Huang, *Adv. Sci.* **2020**, 7, 1903195.
- [9] B. Fei, Z. Chen, J. Liu, H. Xu, X. Yan, H. Qing, M. Chen, R. Wu, *Adv. Energy Mater.* **2020**, 10, 2001963.
- [10] Q. Zhang, N. M. Bedford, J. Pan, X. Lu, R. Amal, *Adv. Energy Mater.* **2019**, 9, 1901312.
- [11] C. Panda, P. W. Menezes, M. Zheng, S. Orthmann, M. Driess, *ACS Energy Lett.* **2019**, 4, 747.
- [12] Y. Zhou, Z. Wang, Z. Pan, L. Liu, J. Xi, X. Luo, Y. Shen, *Adv. Mater.* **2018**, 31, 1806769.
- [13] T. Liu, P. Li, N. Yao, T. Kong, G. Cheng, S. Chen, W. Luo, *Adv. Mater.* **2019**, 31, 1806672.
- [14] G. Yilmaz, C. F. Tan, Y. F. Lim, G. W. Ho, *Adv. Energy Mater.* **2019**, 9, 1802983.
- [15] Y. Yang, H. Yao, Z. Yu, S. M. Islam, H. He, M. Yuan, Y. Yue, K. Xu, W. Hao, G. Sun, H. Li, S. Ma, P. Zapol, M. G. Kanatzidis, *J. Am. Chem. Soc.* **2019**, 141,

- [16] S. Wei, X. Cui, Y. Xu, B. Shang, Q. Zhang, L. Gu, X. Fan, L. Zheng, C. Hou, H. Huang, S. Wen, W. Zheng, *ACS Energy Lett.* **2018**, 4, 368.
- [17] T. L. L. Doan, D. T. Tran, D. C. Nguyen, D. H. Kim, N. H. Kim, J. H. Lee, *Adv. Funct. Mater.* **2020**, 31, 2007822.
- [18] G. Zhou, M. Li, Y. Li, H. Dong, D. Sun, X. Liu, L. Xu, Z. Tian, Y. Tang, *Adv. Funct. Mater.* **2019**, 30, 1905252.
- [19] Z. Kang, H. Guo, J. Wu, X. Sun, Z. Zhang, Q. Liao, S. Zhang, H. Si, P. Wu, L. Wang, Y. Zhang, *Adv. Funct. Mater.* **2019**, 29, 1807031.
- [20] H. Huang, S. Zhou, C. Yu, H. Huang, J. Zhao, L. Dai, J. Qiu, *Energy Environ. Sci.* **2020**, 13, 545.
- [21] M. Zhao, W. Li, J. Li, W. Hu, C. M. Li, *Adv. Sci.* **2020**, 7, 2001965.
- [22] Q. Shi, Q. Liu, Y. Ma, Z. Fang, Z. Liang, G. Shao, B. Tang, W. Yang, L. Qin, X. Fang, *Adv. Energy Mater.* **2020**, 10, 1903854.
- [23] L. Huang, D. Chen, G. Luo, Y. R. Lu, C. Chen, Y. Zou, C. L. Dong, Y. Li, S. Wang, *Adv. Mater.* **2019**, 31, 1901439.
- [24] H. Xu, B. Fei, G. Cai, Y. Ha, J. Liu, H. Jia, J. Zhang, M. Liu, R. Wu, *Adv. Energy Mater.* **2019**, 10, 1902714.
- [25] Z. Zhang, X. Zhao, S. Xi, L. Zhang, Z. Chen, Z. Zeng, M. Huang, H. Yang, B. Liu, S. J. Pennycook, P. Chen, *Adv. Energy Mater.* **2020**, 10, 2002896.
- [26] Y. Pan, K. Sun, S. Liu, X. Cao, K. Wu, W. C. Cheong, Z. Chen, Y. Wang, Y. Li, Y. Liu, D. Wang, Q. Peng, C. Chen, Y. Li, *J. Am. Chem. Soc.* **2018**, 140, 2610.